Electronic Supplementary Material (ESI) for Journal of Materials Chemistry A.

Conjugated polyelectrolytes for stable perovskite solar cells based on methylammonium lead triiodide

Yong Ryun Kim†[a], Juae Kim†[b], Heejoo Kim[c], Hyungcheol Back[e], Geunjin Kim[d], Ayeong Gu[e], Chang-Yong Nam[f], Ju-Hyeon Kim[g], Hongsuk Suh*[b], Kwanghee Lee*[a,e,g]*

[a] Research Institute for Solar and Sustainable Energies (RISE), Gwangju Institute of Science and Technology (GIST), Gwangju 61005, Republic of Korea

[b] Department of Chemistry and Chemistry Institute for Functional Materials, Pusan National University (PNU), Busan 46241, Republic of Korea

[c] Graduate School of Energy Convergence, Institute of Integrated Technology, Gwangju Institute of Science and Technology (GIST), Gwangju 61005, Republic of Korea

[d] Division of Advanced Materials, Korea Research Institute of Chemical Technology (KRICT), Daejeon 34114, Republic of Korea

[e] Heeger Center for Advanced Materials (HCAM), Gwangju Institute of Science and Technology (GIST), Gwangju 61005, Republic of Korea

[f] Centre for Functional Nanomaterials, Brookhaven National Laboratory (BNL), Upton, New York 11973, United States

[g] School of Materials Science and Engineering, Gwangju Institute of Science and Technology, Gwangju 61005, Republic of Korea

†† Y.R.K. and J.K. contributed equally to this work

Address correspondence to heejook@gist.ac.kr, hssuh@pusan.ac.kr, klee@gist.ac.kr,

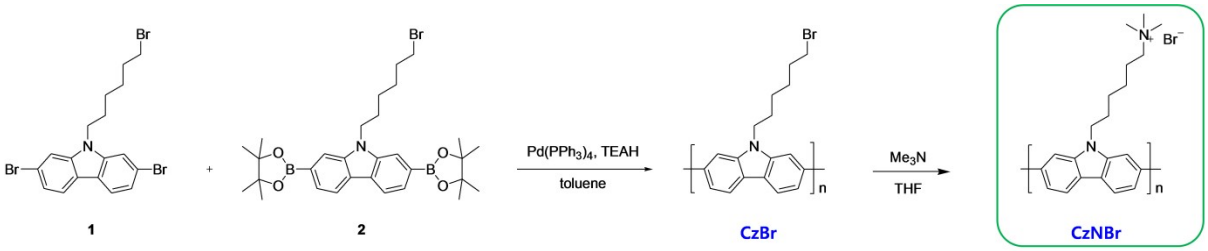

Fig. S1 - Synthetic route of CzNBr.

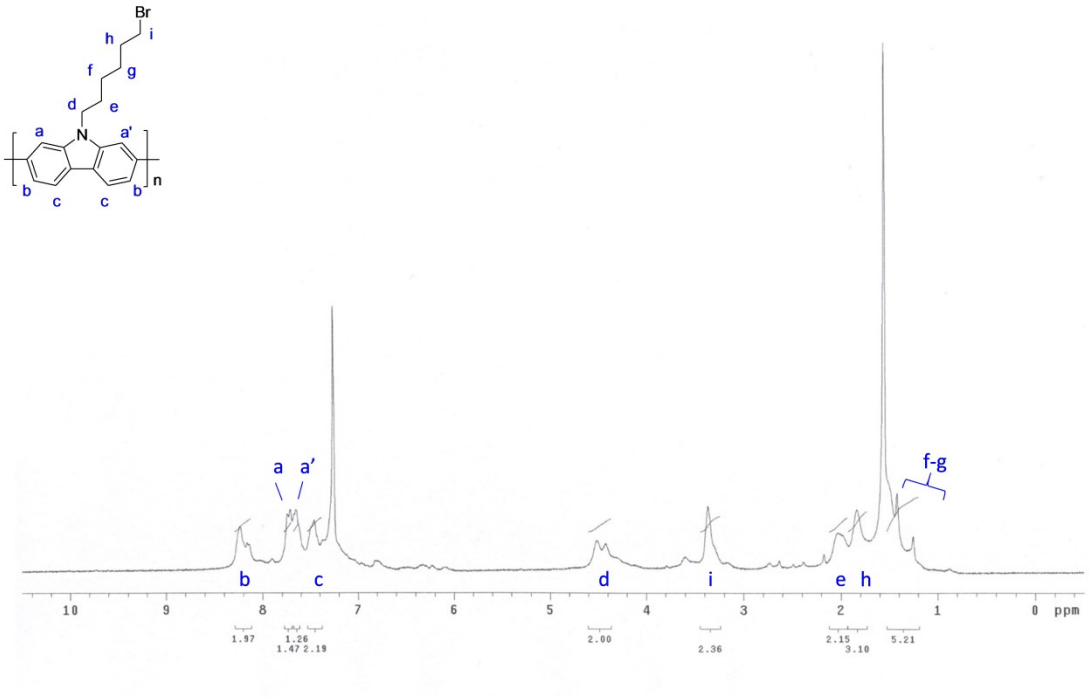

Fig. S2 - ^{1}H NMR of CzB.

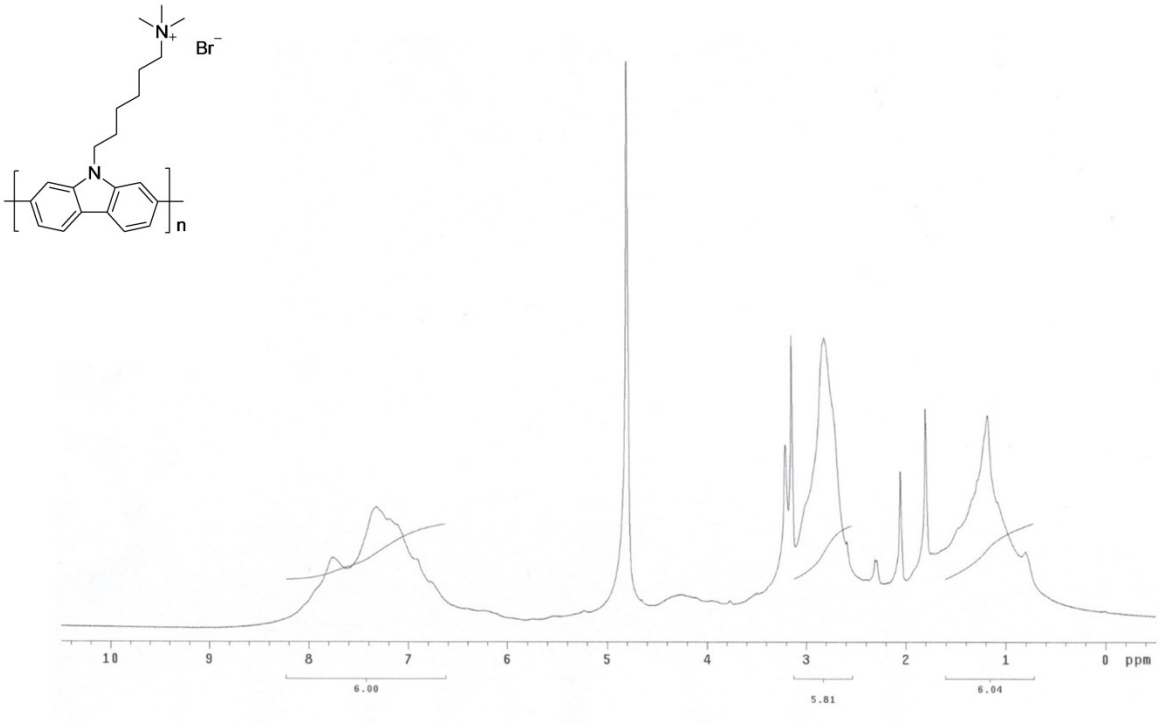

Fig. S3 - ^{1}H NMR of CzNBr.

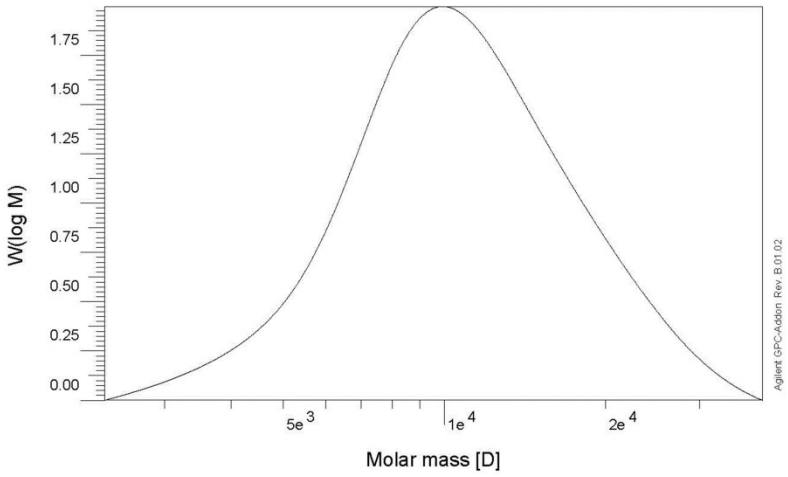

Mn :	9.4337e3	g/mol
Mw :	1.1828e4	g/mol
Mz :	1.4635e4	g/mol
Mv :	0.000000	g/mol
D :	1.2538e0	
[n]:	0.000000	ml/g
Vp :	1.5084e1	ml
Mp :	9.9491e3	g/mol
A :	1.6449e4	ml*V
10%	5.7858e3	g/mol
30%	8.2941e3	g/mol
60%	1.1850e4	g/mol
85%	1.7588e4	g/mol
90%	1.9861e4	g/mol

Fig. S4 - Gel Permeation Chromatography (GPC) data of CzNBr.

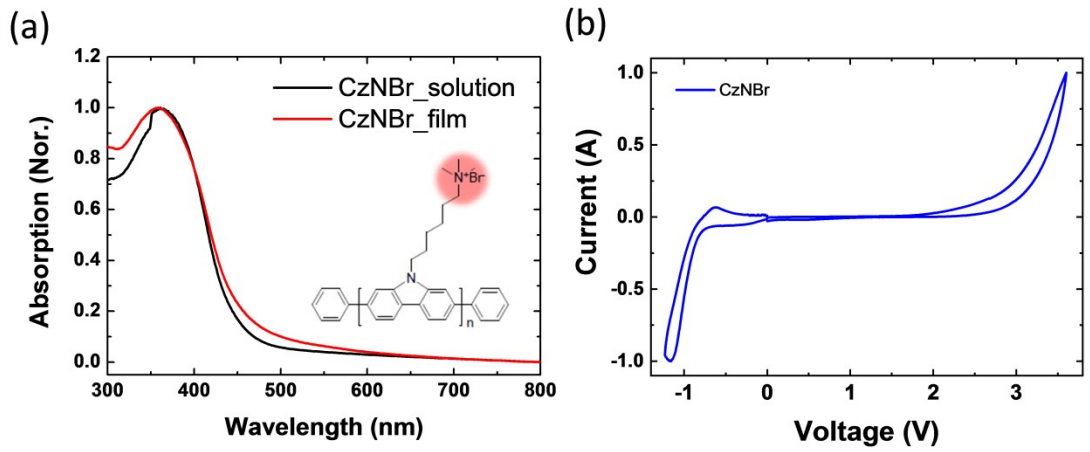

	$\lambda_{max\text{-}solution}$ [a] (nm)	$\lambda_{max\text{-}film}$ (nm) [a]	E_g^{opt}(eV) [b]	HOMO (eV)	LUMO (eV)	E_g^{ele}(eV)
CzNBr	363	360	2.74	-6.79	-3.95	2.84

* $E_{HOMO} = -([E^{onset}]_{ox} + 4.8)$ eV), $E_{LUMO} = -([E^{onset}]_{red} + 4.8)$ eV)

Fig. S5 - Optical and electrochemical characteristics of CzNBr in solution and film.

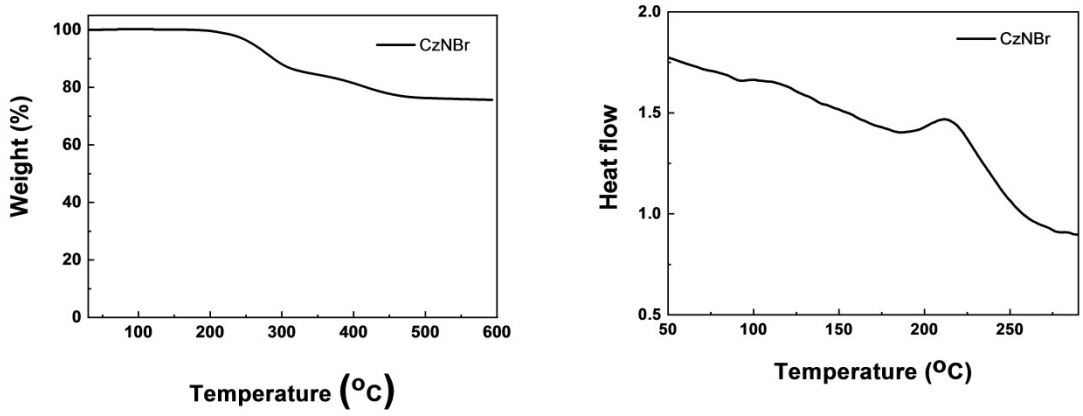

Fig. S6 - Thermogravimetric analysis (TGA) of CzNBr under N_2 conditions.

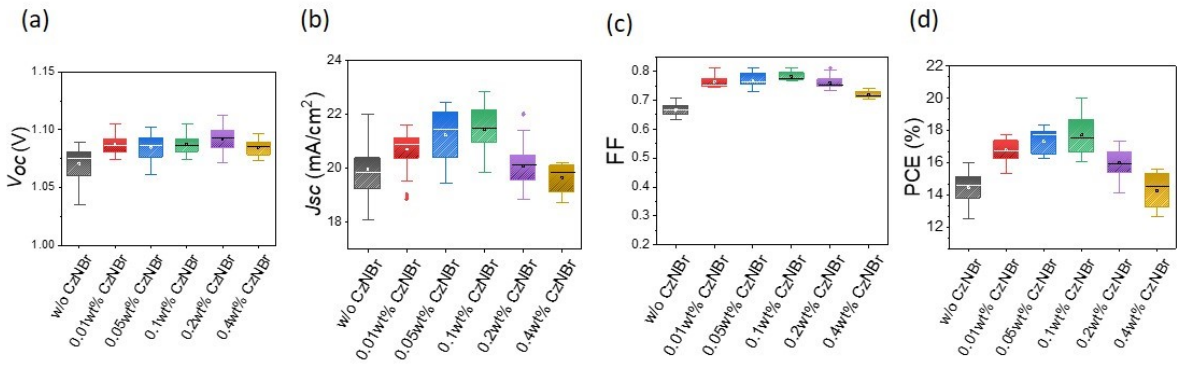

Fig. S7 - Statics of the device parameters depending on various concentrations of CzNBr solution from 0 to 0.4 wt%. (a) The V_{oc}, (b) J_{sc}, (c) FF and (d) PCE were calibrated for 30 devices for each condition.

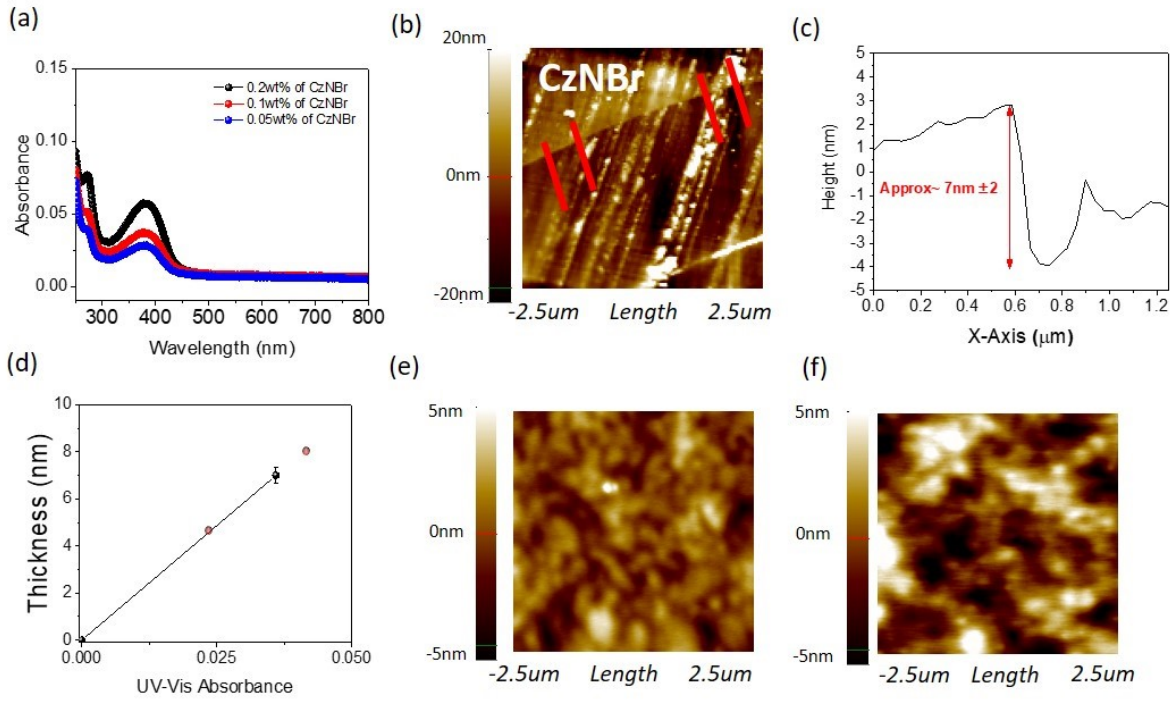

Fig. S8 - (a) UV-Vis spectra of 0.2, 0.1 and 0.05 wt% CzNBr layers deposited on a quartz substrate. (b) AFM images of 0.1 wt% CzNBr deposited on the ITO substrate. (c) The height profiles are measured along the red lines in the corresponding images of (b). (d) shows the estimation of film thickness corresponding to the UV-Vis absorbance of CzNBr according to Beer-lambert's law. (e) and (f) AFM images of the surface morphology corresponding to the structures ITO/PTAA/PFN-Br/$MAPbI_3$/$PC_{61}BM$ and ITO/PTAA/PFN-Br/$MAPbI_3$/$PC_{61}BM$/CzNBr.

(별표 제4호 나-02)

KIER

Test Results

Report No. : KIER-19-0451

Page(3) / (4)Pages

[Appendix 1]

Gwangju Institute of Science and Technology (GIST)
Perovskite solar cell

Device ID : Perov #2
Date of Test : October 25, 2019
Simulator : WACOM, WXS-155S-L2 (Class-AAA)
Reference solar cell : KIER-SS-FD #1
Test condition : STC [AM1.5G, 100 mW/cm^2, (25.0 ± 1.0) °C]

Device Area : 0.155 13 cm^2 (designated illumination area)
Sample Type : Perovskite solar cell (glass plate based)

KIER 한국에너지기술연구원 KOREA INSTITUTE OF ENERGY RESEARCH

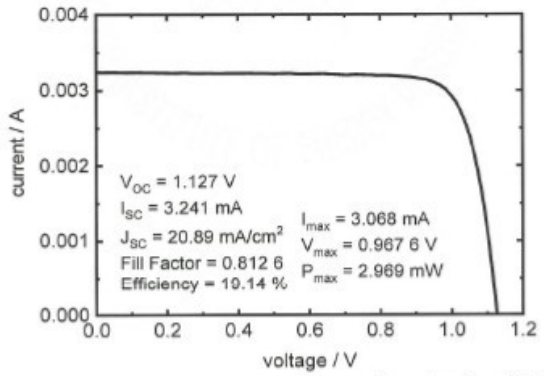

Operator: SangMin Lee

Photovoltaics Laboratory, Korea Institute of Energy Research
152, Gajeong-ro, Yuseong-gu, Daejeon, 34129, Korea
Tel : +82-42-860-3182, e-mail : notask@kier.re.kr

Fig. S9 - Certificated *J-V* characteristics and photovoltaic parameters of CzNBr devices from the Korea Institute of Energy Research (active area of 0.155 cm^2).

	Sweep Direction	J_{sc} (mA/cm^2)	Integrated J_{sc} (mA/cm^2)
w/o CzNBr	FWD	20.75	20.20
	REV	20.67	20.20
w/ CzNBr	FWD	22.70	21.64
	REV	22.78	21.64

Table S1. Summary of J_{sc} values obtained from the *J-V* curve and integrated J_{sc} values from EQE spectra.

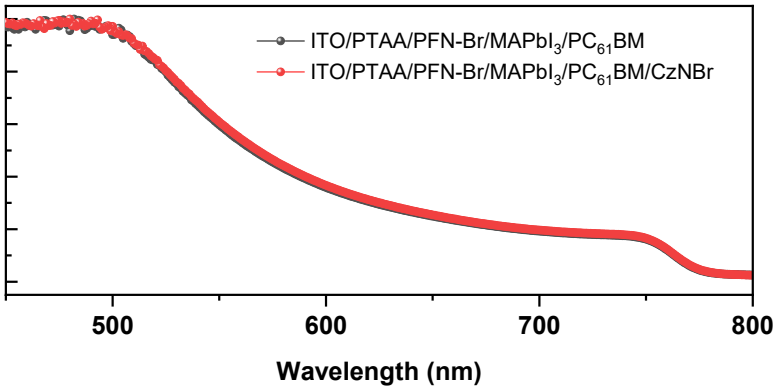

Fig. S10 - (a) UV-Vis spectra of ITO/PTAA/PFN-Br/$MAPbI_3$/$PC_{61}BM$ and ITO/PTAA/PFN-Br/$MAPbI_3$/$PC_{61}BM$/CzNBr.

Table S2. The reported device performance based on pure $MAPbI_3$ with no additives engineering with n-i-p and p-i-n structure.

Device Structure	Metal Electrode	Charge Transport Layer	Hysteresis	J_{sc} (mA/cm^2)	V_{oc} (V)	FF	PCE (%)	ref
N-I-P	Ag	TiO_2/NMTTF	Yes	22.9	1.09	76.5	19.5	1
	Au	SnO_2:Eu^{3+}	Yes	22.57	1.06	77.7	20.1	2
	Au	Lanthanum (La)–doped $BaSnO_3$	Yes	23.4	1.12	81.3	21.2	3
	Au	c-TiO_2/Li-doped m-TiO_2	Yes	21.46	1.05	81.1	18.3	4
	Au	SnO_2	No	22.81	1.07	77.6	18.94	5
P-I-N	Cu	Vacuum processed C60/BCP	Yes (Single Crystal)	23.68	1.14	0.81	21.9	6
	Ag	Vacuum processed /BCP/Bi	No	21.62	1.10	0.76	18.02	7
	Al	Solution processed $PC_{61}BM$(Graphdiyne)ZnO	-	23.3	1.02	78.4	20%	8
	Ag	Solution processed TBAOH-SnO_2	No	21.6	1.08	80.5	18.77	9
	Cu	Solution processed $PC_{61}BM$/BCP	No	21.45	1.09	0.79	18.35	10
	Cu	Vacuum processed C_{60}/BCP	No	22.3	1.07	79	19.1	11
P-I-N	Cu	Solution processed $PC_{61}BM$/CzNBr	No	22.78	1.15	0.80	20.3	Our Work

Reference for Table S2

1. H. Wang, M. Chen, F. Li, R. Sun, P. Wang, F. Ye, H. Zhang, W. Miao, D. Liu and T. Wang, *ACS Applied Energy Materials*, 2020, **3**, 9824-9832.
2. Y. Chen, X. Zuo, Y. He, F. Qian, S. Zuo, Y. Zhang, L. Liang, Z. Chen, K. Zhao, Z. Liu, J. Gou and S. Liu, *Advanced Science*, 2021, **8**, 2001466.
3. S. S. Shin, E. J. Yeom, W. S. Yang, S. Hur, M. G. Kim, J. Im, J. Seo, J. H. Noh and S. I. Seok, *Science*, 2017, **356**, 167-171.
4. P. Holzhey, P. Yadav, S.-H. Turren-Cruz, A. Ummadisingu, M. Grätzel, A. Hagfeldt and M. Saliba, *Materials Today*, 2019, **29**, 10-19.
5. M. B. Johansson, L. Xie, B. J. Kim, J. Thyr, T. Kandra, E. M. J. Johansson, M. Göthelid, T. Edvinsson and G. Boschloo, *Nano Energy*, 2020, **78**, 105346.
6. A. Y. Alsalloum, B. Turedi, X. Zheng, S. Mitra, A. A. Zhumekenov, K. J. Lee, P. Maity, I. Gereige, A. AlSaggaf, I. S. Roqan, O. F. Mohammed and O. M. Bakr, *ACS Energy Letters*, 2020, **5**, 657-662.
7. S. Wu, R. Chen, S. Zhang, B. H. Babu, Y. Yue, H. Zhu, Z. Yang, C. Chen, W. Chen, Y. Huang, S. Fang, T. Liu, L. Han and W. Chen, *Nature Communications*, 2019, **10**, 1161.
8. J. Li, T. Jiu, C. Duan, Y. Wang, H. Zhang, H. Jian, Y. Zhao, N. Wang, C. Huang and Y. Li, *Nano Energy*, 2018, **46**, 331-337.
9. P.-H. Lee, T.-T. Wu, K.-Y. Tian, C.-F. Li, C.-H. Hou, J.-J. Shyue, C.-F. Lu, Y.-C. Huang and W.-F. Su, *ACS Applied Materials & Interfaces*, 2020, **12**, 45936-45949.
10. J.-H. Kim, Y. R. Kim, B. Park, S. Hong, I.-W. Hwang, J. Kim, S. Kwon, G. Kim, H. Kim and K. Lee, *Small*, 2021, **17**, 2005608.
11. X. Wang, K. Rakstys, K. Jack, H. Jin, J. Lai, H. Li, C. S. K. Ranasinghe, J. Saghaei, G. Zhang, P. L. Burn, I. R. Gentle and P. E. Shaw, *Nature Communications*, 2021, **12**, 52.

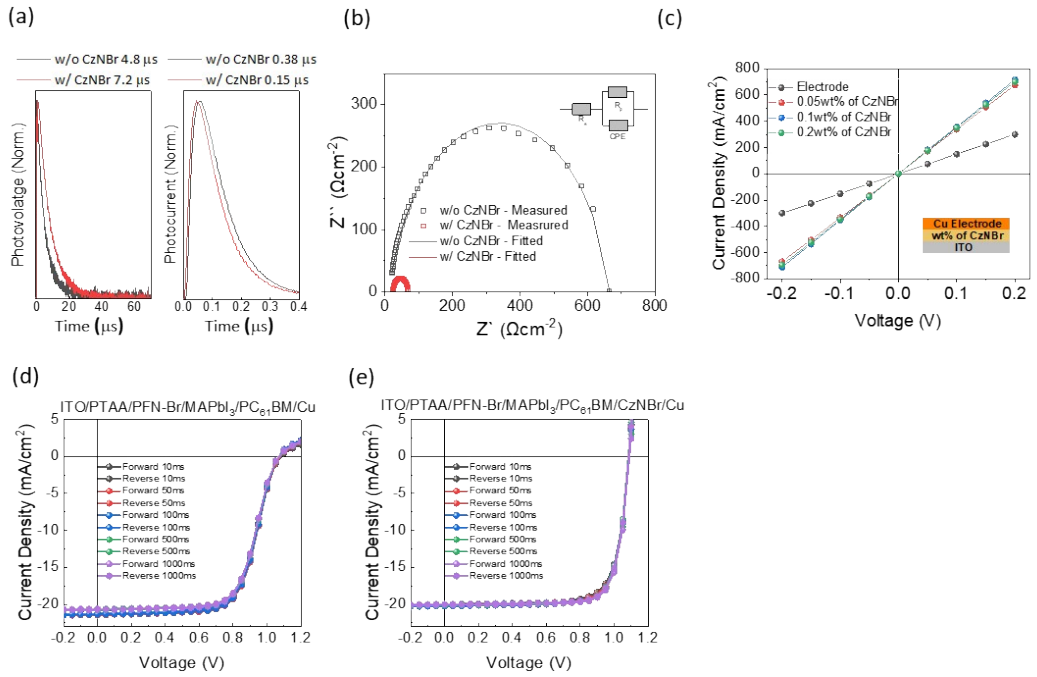

Fig. S11 - (a) Normalized transient photovoltage (TPV, left) and transient photocurrent (TPC, right) decay curves for the I-PSCs with and without CzNBr. (b) Electrochemical impedance spectroscopy (EIS) for I-PSCs with and without CzNBr. Nyquist plots for both devices obtained from the EIS measurement under open-circuit conditions with constant photoirradiation (1 sun, 100 mWcm^{-2}), and the inset shows the fitting of the EIS curve to an equivalent circuit model. (c) Series resistance of J-V curves of the Cu electrode and ITO/0.05, 0.1, and 0.2 wt% of CzNBr/Cu. *J-V* curves for the I-PSC device (d) without and (e) with CzNBr under different scan rates from 10 to 1000 ms.

Table S3. Electrochemical impedance spectroscopy (EIS) measurement fitted parameters for the control and CzNBr devices

	Rp (Ωcm^{-2})	**Rs (Ωcm^{-2})**	**CPE.**
w/o CzNBr	651.40	13.33	0.883
w/ CzNBr	45.14	23.50	0.990

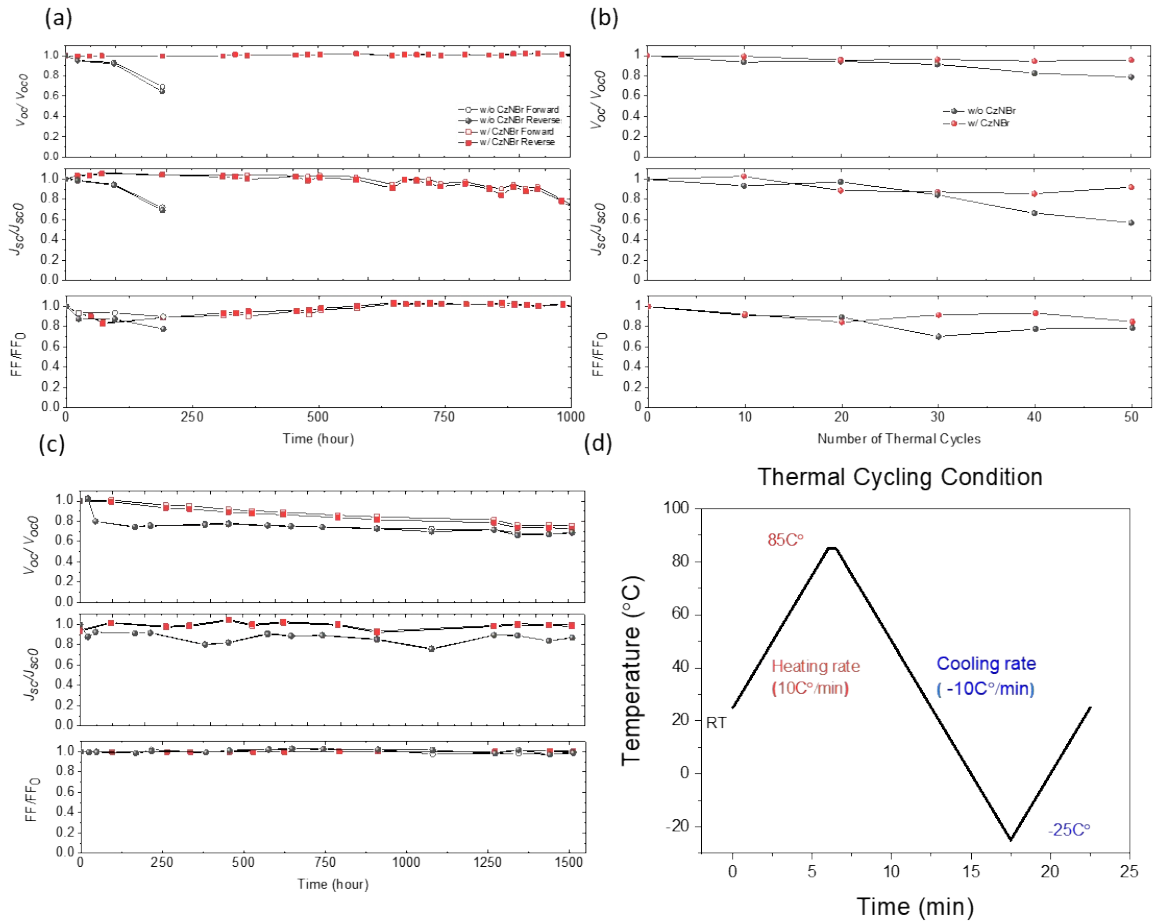

Fig. S12 - Other photovoltaic parameters of the operational stability test of the control and CzNBr device. (a) PCE variations of the control and CzNBr device under continuous thermal annealing at 85°C for 1000 hours under a nitrogen gas atmosphere. (b) PCE variation obtained from the *J-V* characteristics of the control and CzNBr device after a thermal cycling test of 50 cycles at temperatures between -25°C and 85°C (PCE obtained every 10 cycles in ambient air conditions). (c) Environmental stability performance of the control and CzNBr device under ambient conditions (20-40% relative humidity, T = 25°C) and (d) thermal cycling test conditions for one cycle under high vacuum.

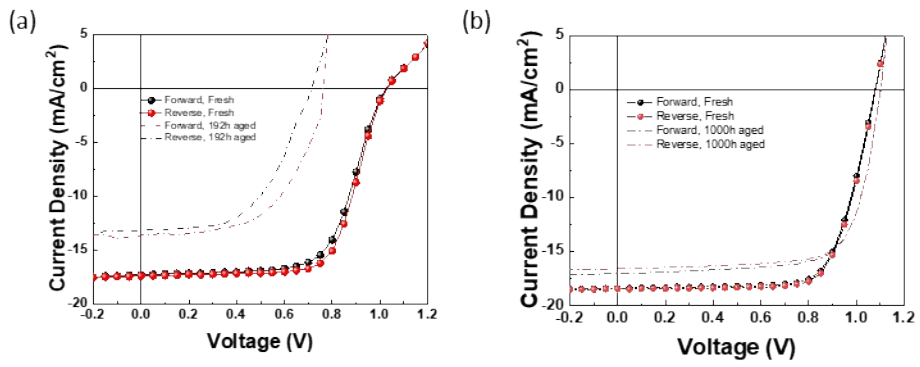

Fig. S13 - *J*-*V* curves for the cases of as-cast and thermally annealed (a) control and (b) CzNBr devices.

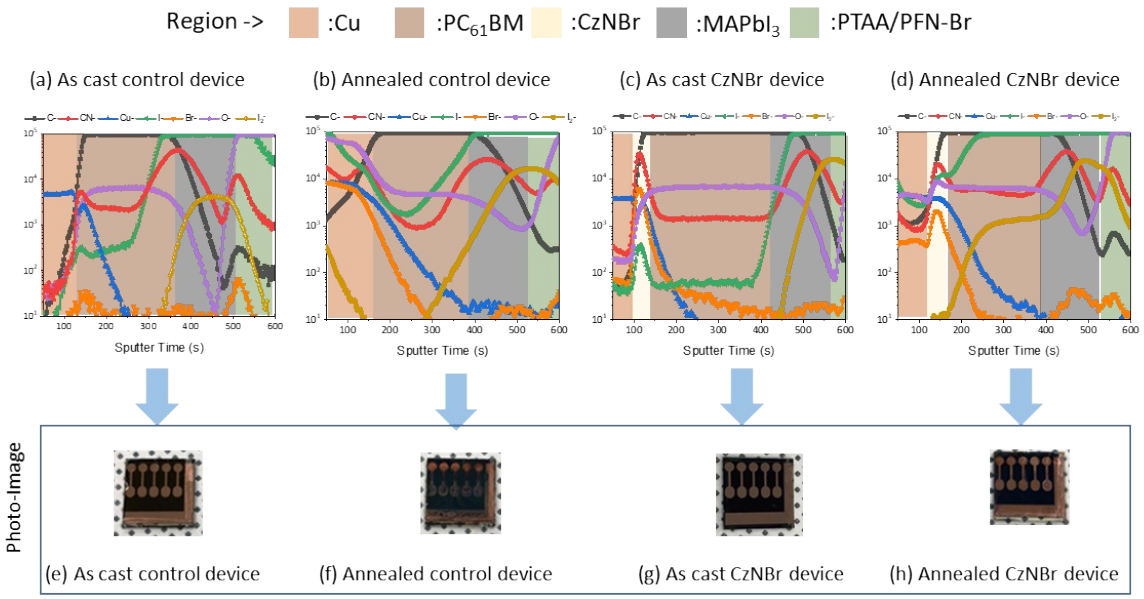

Fig. S14 - ToF-SIMS depth profiles throughout the as-cast and thermally annealed control and CzNBr device. Photographs taken for the control and CzNBr devices before and after 500 h of thermal annealing at 85°C in a N_2-filled glove box. (a), (e) As-cast control device, (b), (f) thermally annealed control device, (c), (g) as-cast CzNBr device and (d), (h) thermally annealed CzNBr device.

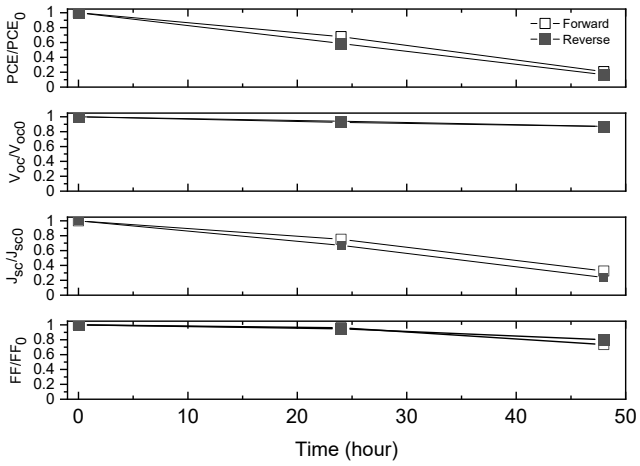

Fig. S15 - The thermal stability test of BCP based device (ITO/PTAA/PFN-Br/$MAPBI_3$/$PC_{61}BM$/BCP/Cu) under continuous thermal annealing at 85°C for 50 hours under a nitrogen gas atmosphere

We tested PSC with BCP layer, which is typically used as cathode buffer layer rather than ion scavenging layer in the inverted PSCs. The only function of BCP layer is a modification of the WF of metal electrode to reduce the interfacial barrier at the interface for effectively charge carrier transport. Therefore, BCP based device exhibited relatively poor thermal stability compared to CzNBr based device.

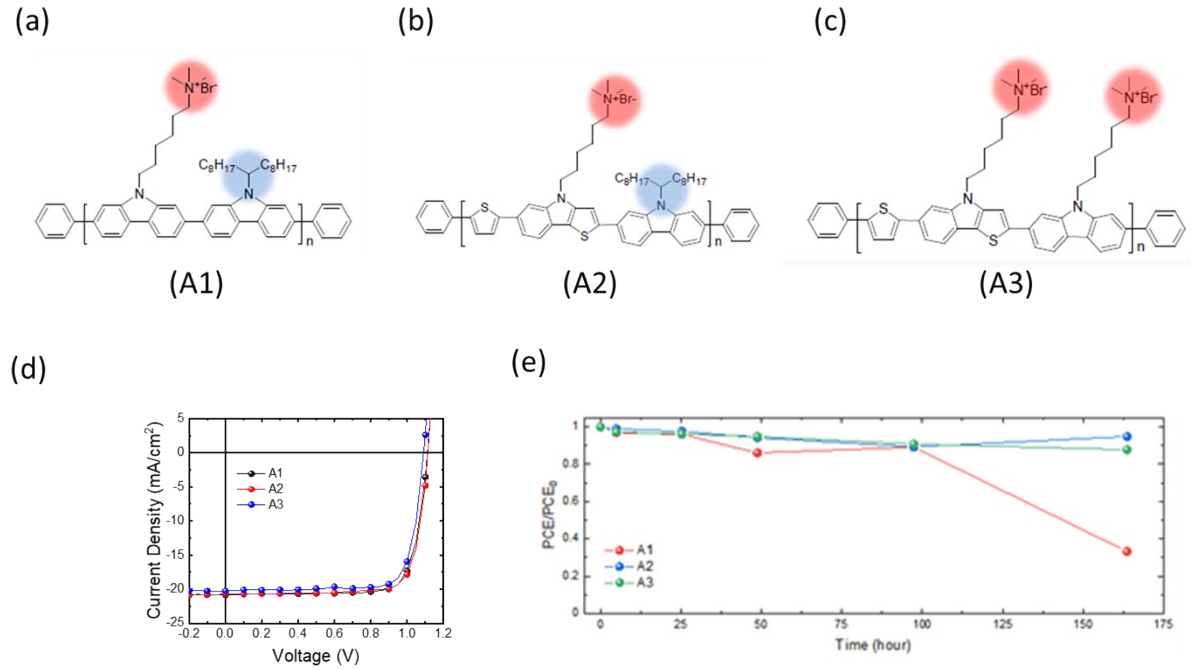

Fig. S16 - (a)-(c) other CPEs (d) J-V curve of PSCs with other CPEs (A1, A2, and A3) (ITO/PTAA/PFN-Br/$MAPBI_3$/$PC_{61}BM$/A1, A2 or A3/Cu) and (e) The thermal stability test under continuous thermal annealing at 85°C for 150 hours under a nitrogen gas atmosphere

Photovoltaic performance of PSCs with other CPEs, which have similar chemical structures with CzNBr (A1, A2, and A3), are compared. Thermal stability test for these devices are also tested. However, the best result was obtained with CzNBr layer.

Table S4. Summary of photovoltaic parameter corresponding to the *J-V* curve of Fig. S16

	Sweep Direction	V_{oc} (V)	J_{sc} (mA/cm^2)	FF (%)	PCE(%)
A1	Forward	1.111	20.82	0.79	18.29
A2	Forward	1.113	20.65	0.80	18.32
A3	Forward	1.090	20.23	0.79	17.43

Device Structure	Perovskite Layer	CTL	Fabrication method for CTL	PCE (%)	Degradation Factors				Ref
					Heat (85℃)	Light		Moisture (air)	
ITO/PTAA/perovskite/C_{60}/BCP/Cu	CsFAMAPbI	C_{60}/BCP/	Vacuum deposition	22.3	1000h in N_2 ※	MPP∞	1000h in N_2*	-	1
FTO/NiO/perovskite/PCBM/BCP/Cr(Cr_2O_3)/Au	CsFAMAPbI	Cr (Cr_2O_3)	Vacuum deposition	19.8	-	Light soaking (76mWcm^{-2})	1800h in air*	-	2
ITO/PEDOT:PSS/perovskite/C_{60}/BCP/Ag	CsSnFAPbI	C_{60}/BCP	Vacuum deposition	16.6	1000h in air※	MPP, Sulphur lamp 0.8 sun	1000h in N_2※	-	3
ITO/PTAA/perovskite/passivation/C_{60}/BCP/Cu	FAMAPbIBr	C_{60}/BCP	Room temperature▽+ Vacuum deposition	21	-	MPP	25h	35 days	4
ITO/NiO_x/perovskite/ZnO/Al	$MAPbI_3$	NiOx	Heat at 300°C for 60min▽	16.1	-	-		60 days	5
ITO/PTAA/perovskite/PCBM/TiOx/Ag	$MAPbI_3$	TiOx	Heat at 100°C for 5min▽	16.09	-	MPP	11h in N_2	200h	6
IT?PEDOT:PSS/perovskite/$PC_{71}BM$/Ca/Al	$MAPbI_3$	Ca/Al	Vacuum deposition	20.1	-	MPP	500s in N_2	30 days*	7
ITO/PTAA/perovskite/PCBM/TiOx/Cu	$MAPbI_3$	TiOx	Vacuum Processing for 100hours	18.8	1000h in N_2	MPP	1000h in N_2	-	8
FTO/NiO/perovskite/PCBM/Ag	$MAPbI_3$	NiOx	Heat at 500°C for 30min	19.19	500h	Light soaking∞	1000h in N_2*	-	9
ITO/PTAA/perovskite//PCBM/C_{60}/BCP/Cu	$MAPbI_3$	C_{60}/BCP	Vacuum deposition	21.1	-	-	-	940h	10
ITO/PTAA/perovskite/PCBM/CzNBr/Cu	$MAPbI_3$	CzNBr	Room temperature▽	20.28	1000h in N_2 (50 cycles for thermal cycling test)	MPP	350h in N_2	1500h	**In this work**

Fig. S17 - Summary of state-of-the-art selected I-PSCs, including PCE and various long-term operational stabilities. Only I-PSCs retaining 80% of their initial PCE are included. For photostability, the illumination source of the xenon lamp was used during measurement unless stated otherwise.

Reference for Fig. S17

1. X. Zheng, Y. Hou, C. Bao, J. Yin, F. Yuan, Z. Huang, K. Song, J. Liu, J. Troughton, N. Gasparini, C. Zhou, Y. Lin, D.-J. Xue, B. Chen, A. K. Johnston, N. Wei, M. N. Hedhili, M. Wei, A. Y. Alsalloum, P. Maity, B. Turedi, C. Yang, D. Baran, T. D. Anthopoulos, Y. Han, Z.-H. Lu, O. F. Mohammed, F. Gao, E. H. Sargent and O. M. Bakr, *Nat. Energy*, 2020, 5, 131-140.

2. S. Bai, P. Da, C. Li, Z. Wang, Z. Yuan, F. Fu, M. Kawecki, X. Liu, N. Sakai, J. T.-W. Wang, S. Huettner, S. Buecheler, M. Fahlman, F. Gao and H. J. Snaith, *Nature*, 2019, 571, 245-250.

3. R. Prasanna, T. Leijtens, S. P. Dunfield, J. A. Raiford, E. J. Wolf, S. A. Swifter, J. Werner, G. E. Eperon, C. de Paula, A. F. Palmstrom, C. C. Boyd, M. F. A. M. van Hest, S. F. Bent, G. Teeter, J. J. Berry and M. D. McGehee, *Nat. Energy*, 2019, 4, 939-947.

4. X. Zheng, B. Chen, J. Dai, Y. Fang, Y. Bai, Y. Lin, H. Wei, Xiao C. Zeng and J. Huang, *Nat. Energy*, 2017, 2, 17102.

5. J. You, L. Meng, T.-B. Song, T.-F. Guo, Y. Yang, W.-H. Chang, Z. Hong, H. Chen, H. Zhou, Q. Chen, Y. Liu, N. De Marco and Y. Yang, *Nat. Nanotech*, 2016, 11, 75-81.

6. H. Back, G. Kim, J. Kim, J. Kong, T. K. Kim, H. Kang, H. Kim, J. Lee, S. Lee and K. Lee, *Energy Enviro. Sci*, 2016, 9, 1258-1263.

7. C.-H. Chiang, M. K. Nazeeruddin, M. Grätzel and C.-G. Wu, *Energy Enviro. Sci,* 2017, 10, 808-817.

8. H. Back, G. Kim, H. Kim, C.-Y. Nam, J. Kim, Y. R. Kim, T. Kim, B. Park, J. R. Durrant and K. Lee, *Energy Enviro. Sci,* 2020, DOI: 10.1039/C9EE03736E.

9. Y. Wu, F. Xie, H. Chen, X. Yang, H. Su, M. Cai, Z. Zhou, T. Noda and L. Han, *Adv. Mater*, 2017, 29, 1701073.

10. M. Zhang, Q. Chen, R. Xue, Y. Zhan, C. Wang, J. Lai, J. Yang, H. Lin, J. Yao, Y. Li, L. Chen and Y. Li, *Nat. Commun*, 2019, 10, 4593.sq